

Available online at [www.sciencerepository.org](http://www.sciencerepository.org)

Science Repository



## Research Article

# Epigenetic Silencing of TMEM176A Activates ERK Signaling in Human Lung Cancer

Hongxia Li<sup>1,2</sup>, Tao He<sup>3</sup>, Fuyou Zhou<sup>4</sup>, James G Herman<sup>5</sup>, Liming Hu<sup>1\*</sup> and Mingzhou Guo<sup>2\*</sup>

<sup>1</sup>College of Life Science and Bioengineering, Beijing University of Technology, Beijing, China

<sup>2</sup>Department of Gastroenterology & Hepatology, Chinese PLA General Hospital, Beijing, China

<sup>3</sup>Department of Pathology, Characteristic Medical Center of the Chinese People's Armed Police Force, Tianjin, China

<sup>4</sup>Department of Thoracic Surgery, Anyang Tumor Hospital, Anyang, China

<sup>5</sup>The Hillman Cancer Center, University of Pittsburgh Cancer Institute, Pittsburgh, Pennsylvania, USA

## ARTICLE INFO

## Article history:

Received: 20 March, 2020

Accepted: 4 April, 2020

Published: 9 April, 2020

## Keywords:

TMEM176A

DNA methylation

NSCLCs

ERK signaling

## ABSTRACT

**Background:** The function of TMEM176A in human lung cancer remains to be elucidated.

**Materials & Methods:** Nine cell lines and 123 cases of lung cancers were employed.

**Results:** TMEM176A was highly expressed in H727 cells, reduced expression was observed in A549, H446 and H460 cells, loss of expression was found in H157, H1563, H358, H1299 and H23 cells. TMEM176A was unmethylated in H727 cells, partially methylated in A549, H446 and H460 cells, and fully methylated in H157, H1563, H358, H1299 and H23 cells. Loss of/reduced expression of TMEM176A is correlated to promoter region methylation. Restoration of TMEM176A expression was induced by 5-AZA-2-deoxycytidine in complete methylated cells, increased expression of TMEM176A was observed in partially methylated cells. These results suggest that TMEM176A is regulated by promoter region methylation in lung cancer cells. TMEM176A was methylated in 53.66% (66/123) of non-small cell lung cancers (NSCLCs) samples. Reduced expression of TMEM176A was associated with promoter region methylation in 40 cases of matched primary NSCLCs and adjacent tissue samples ( $P < 0.05$ ). TMEM176A expression induced cell apoptosis, inhibited colony formation, cell proliferation, migration and invasion.

**Conclusion:** Methylation of TMEM176A activated ERK signaling in lung cancer cells. TMEM176A suppressed human lung cancer cell xenograft growth in mice.

© 2020 Mingzhou Guo & Liming Hu. Hosting by Science Repository. All rights reserved.

## Introduction

Lung cancer is one of the most common cancers and the leading cause of cancer related death worldwide [1]. Tobacco consumption is considered the most important risk factor for the development of lung cancer [2], while it is currently well established that an important percentage of never smokers are diagnosed with lung cancer [3]. Many other risk factors have been described, including radon, asbestos exposure, domestic fuel smoke and HPV infection [2, 3]. The mechanism of lung cancer development remains unclear. Aberrant

genetic and epigenetic changes are involved in tumorigenesis and progression [4, 5].

The identification of actionable oncogenic mutations has greatly improved the treatment of different cancers [6-8]. In non-small cell lung cancers (NSCLCs), the discovery of activating mutations in the epidermal growth factor receptor (EGFR) gene have ushered in a new era of genomics-guided precision targeted therapy in lung cancer [9]. Advances in the knowledge of pathway, newly developed drugs to block the activities of the pathways in recent years have allowed the physicians to tailor the treatment options [8, 10]. Nevertheless, this unprecedented

\*Correspondence to: Mingzhou Guo, Department of Gastroenterology & Hepatology, Chinese PLA General Hospital, #28 Fuxing Road, Beijing 100853, China; Tel: +861066937651; Fax: +861068180325; E-mail: mzguo@hotmail.com

Liming Hu, College of Life Science and Bioengineering, Beijing University of Technology, Beijing 100124, China; E-mail: huliming@bjut.edu.cn

benefit from current standard therapies is still observed in only a minority of patients.

Aberrant epigenetic changes have been reported in various cancers, including lung cancer [4, 5, 11, 12]. Cancer-related signaling pathways may be disrupted by a key component aberrant methylation. Novel epigenome-based therapeutic strategies are developing, including “synthetic lethality” [10].

Human transmembrane protein 176A (TMEM176A) was first identified by screening tumor related antigens in hepatocellular carcinoma (HCC) [13, 14]. Most of studies were mainly focused on its function in development and the immune system [15-17]. In our previous study, the expression of TMEM176A was reduced in human CRC tissue samples compared to normal colorectal mucosa, according to RNA-seq [18]. TMEM176A was found frequently methylated in human colorectal, hepatic and esophageal cancers and may serve as a tumor suppressor [18-20]. The expression regulation and the mechanism of TMEM176A in lung cancer remain to be elucidated.

## Materials and Methods

### I Human tissue samples and cell lines

Primary lung cancer samples (90) were collected from the Chinese PLA General Hospital and 33 primary samples were collected from the tumor hospital of Henan. The median age of the cancer patients was 60 years (range from 29 to 79). Fifteen cases of normal lung tissue were collected from the Chinese PLA General Hospital. Among 123 cancer samples, only 40 cases were available for paraffin samples with matched cancer and adjacent tissue. All samples were collected following the guidelines approved by the Institutional Review Board of the Chinese PLA General Hospital and the tumor hospital of Henan with written informed consent from patients. Nine lung cancer cell lines (H727, H157, H1563, H358, H446, H460, H23, H1299 and A549) purchased from American Type Culture Collection (ATCC) and grown in RPMI-1640 (Invitrogen, Carlsbad, CA, USA) supplemented with 10% fetal bovine serum (Hyclone, Logan, UT) and 1% penicillin/streptomycin solution (Sigma, St. Louis, MO).

### II 5-Aza-2-Deoxycytidine and SCH772984 Treatment

For methylation regulation analysis, lung cancer cell lines were split to low density (30% confluence) 12 hours before treatment. Cells were treated with 5-Aza-2'-deoxycytidine (DAC, Sigma, St. Louis, MO, USA) at a concentration of 2  $\mu$ M in the growth medium, which was exchanged every 24 hours for a total of 96 hours and cultured at 37°C in a 5% CO<sub>2</sub> incubator. At the end of the treatment period, cells were prepared for the extraction of total RNA. To verify the role of TMEM176A in ERK signaling, SCH772984, an ERK inhibitor, was added to TMEM176A knocking down H727 cell at 2 $\mu$ m for 24h (MedChemExpress, Monmouth Junction, USA) [21].

### III RNA Isolation and Semi-Quantitative RT-PCR

Total RNA was extracted using Trizol Reagent (Life Technologies, Carlsbad, CA, USA). Agarose gel electrophoresis and

spectrophotometric analysis were used to detect RNA quality and quantity. The first strand cDNA was synthesized according to the manufacturer's instructions (Invitrogen, Carlsbad, CA). A total of 5 $\mu$ g RNA was used to synthesize the first strand cDNA. The reaction mixture was diluted to 100 $\mu$ l with water, and then 2 $\mu$ l of diluted cDNA was used for 25 $\mu$ l PCR reaction. The PCR primer sequences for TMEM176A were as follows: 5'-GGGAACAG CCG ACA G TGAT-3' (F) and 5'-GCC AGC GTT AGCAGAGTCCT-3'(R). PCR cycle conditions were as follows: 95°C 5 min, 1 cycle; (95°C 30 s, 60°C 30 s and 72°C 30 s) 32 cycles; 72°C 5 min, 1 cycle. PCR product size is 369bp. GAPDH was amplified for 25 cycles as an internal control. The GAPDH primer sequences were as follows: 5'-GACCAC AGT CCA TGC CAT CAC-3' (F), and 5'-GTC CACCAC CCT GTT GCT GTA-3' (R). PCR cycle conditions were as follows: 95°C 5 min, 1 cycle; (95°C 30 s, 63°C 30 s and 72°C 30 s) 25cycles; 72°C 5 min, cycle. PCR product size is 448bp. The amplified PCR products were examined by 2% agarose gels.

### IV DNA Extraction, Bisulfite Modification, Methylation-Specific PCR (MSP)

Genomic DNA from lung cancer cell lines and lung cancer tissue samples were prepared using the proteinase-K method. Normal lymphocyte DNA was prepared from healthy donor blood lymphocytes by proteinase-K method [22]. Normal lymphocyte DNA (NL) was used as a control for unmethylation and in vitro methylated DNA (IVD) was used as a methylation control. IVD was prepared using SssI methylase (New England Biolabs, Ipswich, MA, USA) following the manufacturer's instructions. MSP primers were designed according to genomic sequences inside the CpG islands in the TMEM176A gene promoter region.

MSP primers for TMEM176A were designed -364 to -203bp upstream of the transcription start site (TSS) and synthesized to detect methylated (M) and unmethylated (U) alleles. The detected region has been previously reported to be hypermethylated and associated with low expression [23]. MSP primers for TMEM176A were as follows: 5'-GTT TCG TTT AGG TTG CGC GGT TTT TC -3' (MF), 5'-CCA AAA CCG ACG TAC AAA TAT ACG CG-3' (MR); 5'-TGG TTT TGT TTA GGT TGT GTG GTT TTT T-3' (UF), 5'-CAA CCA AAA CCA ACA TAC AAA TAT ACA CA -3' (UR). PCR cycle conditions were as follows: 95°C 5 min, 1 cycle; (95°C 30 s, 60°C 30 s and 72°C 30 s) 35cycles; 72°C 5 min, 1 cycle.

Bisulfite sequencing (BSSQ) primers encompassed a 231bp region upstream of the TMEM176A transcription start site (-388bp to -157bp) and included the region analyzed by MSP. BSSQ primers were designed as follows: 5'-GAG ACG GTA GAT GTA CGG GT-3' (F); 5'- AAC RAA CRA CCC TAA AAA AAC CC -3' (R). PCR cycle conditions were as follows: 95°C 5 min, 1 cycle; (95°C 30 s, 55°C 30 s and 72°C 30 s) 35cycles; 72°C 5 min, 1 cycle.

### V Immunohistochemistry

Immunohistochemistry (IHC) was performed in primary lung cancer samples and matched adjacent tissue samples. TMEM176A antibody was diluted to 1:50 (Cat: HPA008770, Sigma, St. Louis, MO, USA). The expression of MMP2 and MMP9 was detected in H1299 cell xenografts.

MMP2 and MMP9 antibody was diluted to 1:100 and 1:100 (Protein Tech Group, Chicago, IL, USA). The procedure was performed as described previously [24]. The staining intensity and extent of the staining area were scored using the German semi-quantitative scoring systems as previously described [24-26]. Staining intensity of the membrane and/or cytoplasm was characterized as follows: no staining = 0, weak staining = 1, moderate staining = 2, strong staining = 3; the extent of staining was defined as: 0% = 0, 1-24% = 1, 25-49% = 2, 50-74% = 3, 75-100% = 4. The final immune-reactive score (0-12) was determined by multiplying the intensity score by the extent of the staining score.

## VI Construction of Lentiviral TMEM176A Expression Vectors and Selection of Stable Expression Cells

The human full-length TMEM176A cDNA (NM-018487.2) was cloned into the pLenti6 vector. Primers were as follows: 5'-CTT AGG ATC CGC CAC CAT GGG AAC AGC CGAC -3' (F) and 5'-ACT TAG TCG ACC TAG ATT CCA CTC ACT TCC -3' (R). The HEK-293T cell line was maintained in DMEM (Invitrogen, CA, USA) supplemented with 10% fetal bovine serum. TMEM176A expressing Lentiviral vector was transfected into HEK-293T cells ( $5.5 \times 10^6$  per 100 mm dish) using Lipofectamine 3000 Reagent (Invitrogen, Carlsbad, CA, USA) at a ratio of 1:3 (DNA mass: Lipo mass). Viral supernatant was collected and filtered after 48 hours. H23 and H1299 cells were then infected with viral supernatant. H23 and H1299 cells stably expressing TMEM176A were selected with Blasticidin (Life Technologies, Carlsbad, CA, USA) at concentrations of 6.0  $\mu\text{g/ml}$  and 5.0  $\mu\text{g/ml}$  for 2 weeks, respectively.

## VII RNA Interference Assay

Two sets of targeting siRNA for TMEM176A and one set of RNAi negative control duplex sequence are as follows: SiTMEM176A1 duplex (sense: 5'-GGC UAC UCU UAU UAC AAC ATT-3'; antisense: UGU UGU AAU AAG AGU AGC CTT-3'), SiTMEM176A2 duplex (sense: 5'-CUG UAC UGC UGG AGA AUG UTT-3'; antisense: 5'-ACA UUC UCC AGC AGU ACA GTT-3'), SiTMEM176A negative control duplex (SiTMEM176ANC, sense: 5'-ACA UUC UCC AGC AGU ACA GTT-3'; antisense: 5'-ACG UGA CAC GUU CGG AGA ATT-3'). SiTMEM176A2 was found more effective than SiTMEM176A1, and SiTMEM176A2 was applied to further study (GenePharma Co. Shanghai, China).

## VIII Cell Viability Detection

H23 and H1299 cells were seeded into 96-well plates before and after re-expression of TMEM176A at  $1 \times 10^3$  cells/well. H727 cell were plated into 96-well plates before and after knockdown of TMEM176A at a density of  $5 \times 10^3$  cells/well. The cell viability was measured by MTT (3-(4,5-dimethylthiazol-2-yl)-2,5-diphenyltetrazoliumbromide) assay at 0h, 24h, 48h, 72h, 96h (KeyGENBiotech, Nanjing, China). Absorbance was measured on a microplate reader (Thermo Multiskan MK3, MA, USA) at a wavelength of 490nm. Each experiment was repeated three times.

## IX Colony Formation Assay

TMEM176A stably re-expressed and unexpressed H23 and H1299 cells were plated onto 6-well plates at a density of 200 cells per well. H727 cells before and after knockdown of TMEM176A were seeded in 6-well plates at a density of 300 cells per well. After 2 weeks, cells were fixed with 75% ethanol for 30 min. Colonies were then stained with 0.5% crystal violet solution and counted. The experiment was performed in triplicate.

## X Flow Cytometry

To increase the sensitivity of apoptosis detection, TMEM176A stably unexpressed and re-expressed H23 and H1299 cells were treated with Doxorubicin at 0.8  $\mu\text{g/ml}$  and 0.6  $\mu\text{g/ml}$  for 24 hours respectively [27]. Apoptosis was also analyzed in H727 cells with or without knockdown of TMEM176A. The cells were prepared using the FITC Annexin V Apoptosis Detection Kit I (BD Biosciences, Franklin Lakes, NJ, USA) following the manufacturer's instructions and then sorted by FACS Calibur (BD Biosciences, Franklin Lakes, NJ, USA). Each experiment was repeated three times.

## XI Transwell Assay

Migration:  $5 \times 10^4$  TMEM176A unexpressed and re-expressed H23 and  $2 \times 10^4$  H1299 cells were suspended in 200  $\mu\text{l}$  serum-free RPMI 1640 media and added to the upper chamber of an 8.0  $\mu\text{m}$  pore size transwell apparatus (COSTAR Transwell Corning Incorporated, Tewksbury, MA, USA). Cells that migrated to the lower surface of the membrane were stained with crystal violet and counted in three independent high-power fields ( $\times 100$ ) after incubation for 16 hours (H23 cells) or 16 hours (H1299). Each experiment was repeated three times.

Invasion: the top chamber was coated with a layer of extracellular matrix. H23 cells ( $1 \times 10^5$ ) and H1299 cells ( $5 \times 10^4$ ) were seeded to the upper chamber of a transwell apparatus coated with Matrigel (BD Biosciences, CA, USA) and incubated for 36 hours (H23) and 36 hours (H1299). Each experiment was repeated three times.

## XII Western Blot

Cells were collected 48h after transfection and cell lysates were prepared using ice-cold Tris buffer (20 mmol/L Tris; pH 7.5) containing 137 mmol/L NaCl, 2 mmol/L EDTA, 1% Triton X, 10% glycerol, 50 mmol/L NaF, 1 mmol/L DTT, PMSF, and a protein phosphatases inhibitor (Applygen Tech. Beijing, China). For extracellular signal-regulated kinase (ERK) signaling analysis, cells were starved with serum-free medium for 24 h after transfection. These cells were then stimulated with medium containing 10% serum for 60 min before collection. Western blot was performed as described previously [24]. Primary antibodies were as follows: TMEM176A (Sigma, St. Louis, MO), cleaved caspase-3 (Protein Tech Group, Chicago, IL, USA), MMP2 (Protein Tech Group, Chicago, IL, USA), MMP9 (Protein Tech Group, Chicago, IL, USA), ERK1/2 (Protein Tech Group, Chicago, IL, USA), p-ERK1/2 (Cell Signaling Technology, Danfoss, MA, USA), SAR1A (Protein Tech Group, Chicago, IL, USA) and  $\beta$ -actin (Beyotime Biotech, Nanjing, China).

**XIII Lung Cancer Cell Xenograft Mouse Model**

H1299 cell lines stably transfected with plenti6 vector or plenti6-TMEM176A vector ( $1 \times 10^7$  cells diluted in phosphate-buffer saline) were injected subcutaneously into the dorsal left side of 4-week-old female Balb/c nude mice. Each group included six mice. Tumor volume was measured every 4 days. Tumor volume was calculated according to the formula:  $V=L \times W^2 / 2$ , in which V represents volume ( $\text{mm}^3$ ), L represents the biggest diameter (mm), and W represents the smallest diameter (mm). Mice were sacrificed on the 24<sup>th</sup> day after inoculation, and the tumors were weighed. All procedures were approved by the Animal Ethics Committee of the Chinese PLA General Hospital.

**XIV Data Analysis**

RNASeq data for TMEM176A gene expression in the dataset of lung cancer and normal tissues were downloaded from the Cancer Genome Atlas (TCGA) (<http://xena.ucsc.edu/>, 09/16/2019). Statistical analysis was performed using SPSS 17.0 software (SPSS, Chicago, IL). Chi-square test was used to evaluate the relationship between methylation status and clinicopathological characteristics. The 2-tailed independent samples t-test was applied to determine the statistical significance of the differences between the two experimental groups. Two-sided tests were used to determine the significance, and  $P < 0.05$  was considered statistically significant.

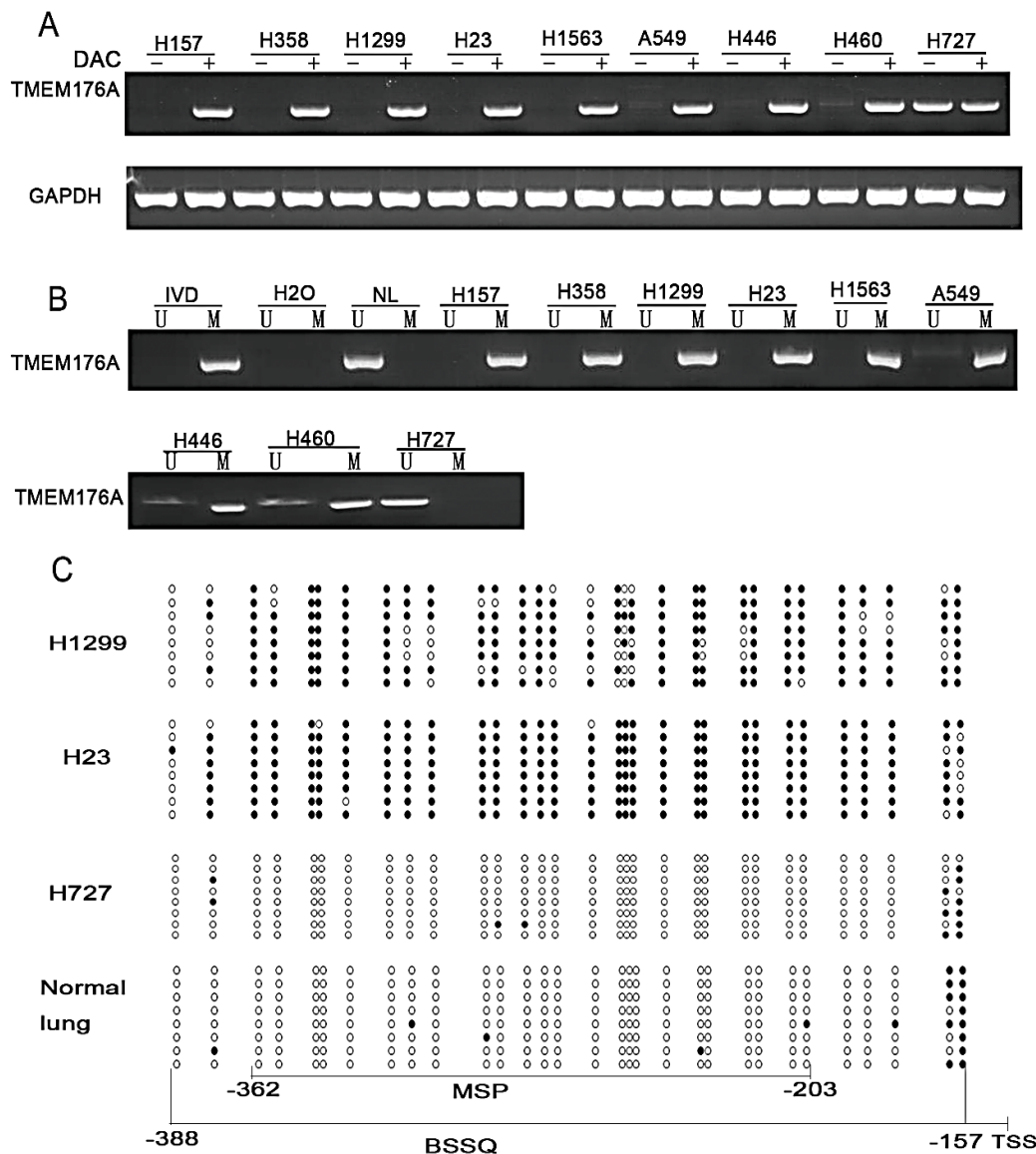


**Figure 1:** TMEM176A expression and methylation status in human lung cancer cells. **A)** Semi-quantitative RT-PCR shows TMEM176A expression levels in lung cancer cell lines. H157, H358, H1299, H23, H1563, A549, H446, H460 and H727 are lung cancer cells. DAC: 5-aza-2'-deoxycytidine; GAPDH: internal control; (-): absence of DAC; (+): presence of DAC. **B)** MSP results of TMEM176A in lung cancer cell lines. U: unmethylated alleles; M: methylated alleles; IVD: in vitro methylated DNA, serves as methylation control; NL: normal peripheral lymphocytes DNA, serves as unmethylated control; H<sub>2</sub>O: double distilled water. **C)** BSSQ results of TMEM176A in H1299, H23, H727 cells and normal lung. MSP PCR product size was 159bp and bisulfite

sequencing focused on a 231bp region of the CpG island (from -388 to -157) around the TMEM176A transcription start site. Filled circles: methylated CpG sites, open circles: unmethylated CpG sites. TSS: transcription start site.

**Results**

**I TMEM176A is Frequently Methylated in Human NSCL Cancer and the Expression of TMEM176A is Regulated by Promoter Region Hypermethylation**

The expression of TMEM176A was examined in human lung cancer cells by semi-quantitative RT-PCR. TMEM176A was highly expressed in H727 cells, reduced expression was observed in A549, H446 and H460 cells, and no expression was found in H157, H1563, H358, H1299 and H23 cells (Figure 1A). The methylation status was examined by methylation-specific PCR (MSP) in the promoter region. Unmethylation was detected in H727 cells, partial methylation was observed in A549, H446 and H460 cells, and complete methylation was found in H157, H1563, H358, H1299 and H23 cells (Figure 1B). These results demonstrate that loss of/reduced expression of TMEM176A was correlated with promoter region methylation.

To further validate that the expression of TMEM176A was regulated by promoter region methylation, lung cancer cells were treated with 5-AZA-2-deoxycytidine. Upon treatment with 5-AZA-2-deoxycytidine,

re-expression of TMEM176A was found in H157, H1563, H358, H1299 and H23 cells, increased expression of TMEM176A was observed in A549, H446 and H460 cells, and no expression changes were found in H727 cell before and after treatment (Figure 1A). These results suggest that the expression of TMEM176A is regulated by promoter region methylation in lung cancer cells. To further validate the efficiency of MSP primers and explore the methylation density in lung cancer, sodium bisulfite sequence (BSSQ) was performed in H1299, H23, H727 cells and normal lung tissue samples. Dense methylation was observed in the promoter region of TMEM176A in H1299 and H23 cells, unmethylation was detected in H727 cells and normal lung tissue samples (Figure 1C).

The methylation status of TMEM176A was also detected by MSP in 123 cases of primary human lung cancer and 15 cases of non-cancerous lung tissue samples. TMEM176A was methylated in 53.66% (66/123) of human primary lung cancer, and no methylation was found in non-cancerous lung tissue samples (Figure 2A). No association was found between TMEM176A methylation and age, gender, alcohol abuse, smoking, tumor size, lymph node metastasis, differentiation and TNM stage (Table 1, all  $P > 0.05$ ).

**Table 1:** The association of TMEM176A methylation and clinical factors in NSCLC.

| Clinical factor       | No. | TMEM176A methylation status |                          | *P-value |
|-----------------------|-----|-----------------------------|--------------------------|----------|
|                       |     | Unmethylated n=57 (46.34%)  | Methylated n=66 (53.66%) |          |
| Age (year)            |     |                             |                          | 0.412    |
| <60                   | 62  | 31                          | 31                       |          |
| ≥60                   | 61  | 26                          | 35                       |          |
| Gender                |     |                             |                          | 0.879    |
| Male                  | 92  | 43                          | 49                       |          |
| Female                | 31  | 14                          | 17                       |          |
| Smoking               |     |                             |                          | 0.529    |
| Yes                   | 77  | 35                          | 42                       |          |
| No                    | 46  | 23                          | 23                       |          |
| Alcohol abuse         |     |                             |                          | 0.125    |
| Yes                   | 41  | 15                          | 26                       |          |
| No                    | 82  | 42                          | 40                       |          |
| Tumor size (cm)       |     |                             |                          | 0.137    |
| >5                    | 12  | 8                           | 4                        |          |
| ≤5                    | 111 | 49                          | 62                       |          |
| Differentiation       |     |                             |                          | 0.196    |
| Well                  | 24  | 14                          | 10                       |          |
| Moderate              | 73  | 29                          | 44                       |          |
| Poor                  | 26  | 14                          | 12                       |          |
| TNM stage             |     |                             |                          | 0.468    |
| Stage I               | 41  | 17                          | 24                       |          |
| Stage II              | 41  | 23                          | 18                       |          |
| Stage III             | 35  | 15                          | 20                       |          |
| Stage IV              | 6   | 2                           | 4                        |          |
| Lymph node metastasis |     |                             |                          | 0.646    |
| Negative              | 62  | 30                          | 32                       |          |
| Positive              | 61  | 27                          | 34                       |          |

\*P values are obtained from chi-square test.

The expression of TMEM176A was evaluated by immunohistochemistry in 40 cases of available matched lung cancer and



adjacent tissue samples. TMEM176A staining was found mainly in the cytoplasm and cell membranes (Figure 2B). The expression levels of TMEM176A were reduced in cancer compared to adjacent tissue samples (Figure 2C, Student's t-distribution (t-test),  $P < 0.05$ ). Lower level expression of TMEM176A was found in 35 cases (Figure 2D). Among the 35 cases that had reduced expression of TMEM176A, 20 cases were methylated (Figure 2D). These data indicate that the expression of TMEM176A is regulated by promoter region methylation in human primary lung cancer.

The Cancer Genome Atlas (TCGA) database was employed to further validate that the expression of TMEM176A is regulated by promoter region methylation. TMEM176A mRNA expression and promoter region methylation data were extracted from the TCGA database (<http://xena.ucsc.edu/>). The methylation of TMEM176A (cg19336959) was analyzed by Illumina Infinium Human Methylation 450 (HM450). In the 457 cases of lung adenocarcinoma samples and 372 cases of lung squamous carcinoma samples, reduced expression of TMEM176A was associated with promoter region hypermethylation (Figures 2E & 2F). These data further suggested that the expression of TMEM176A is regulated by promoter region methylation.

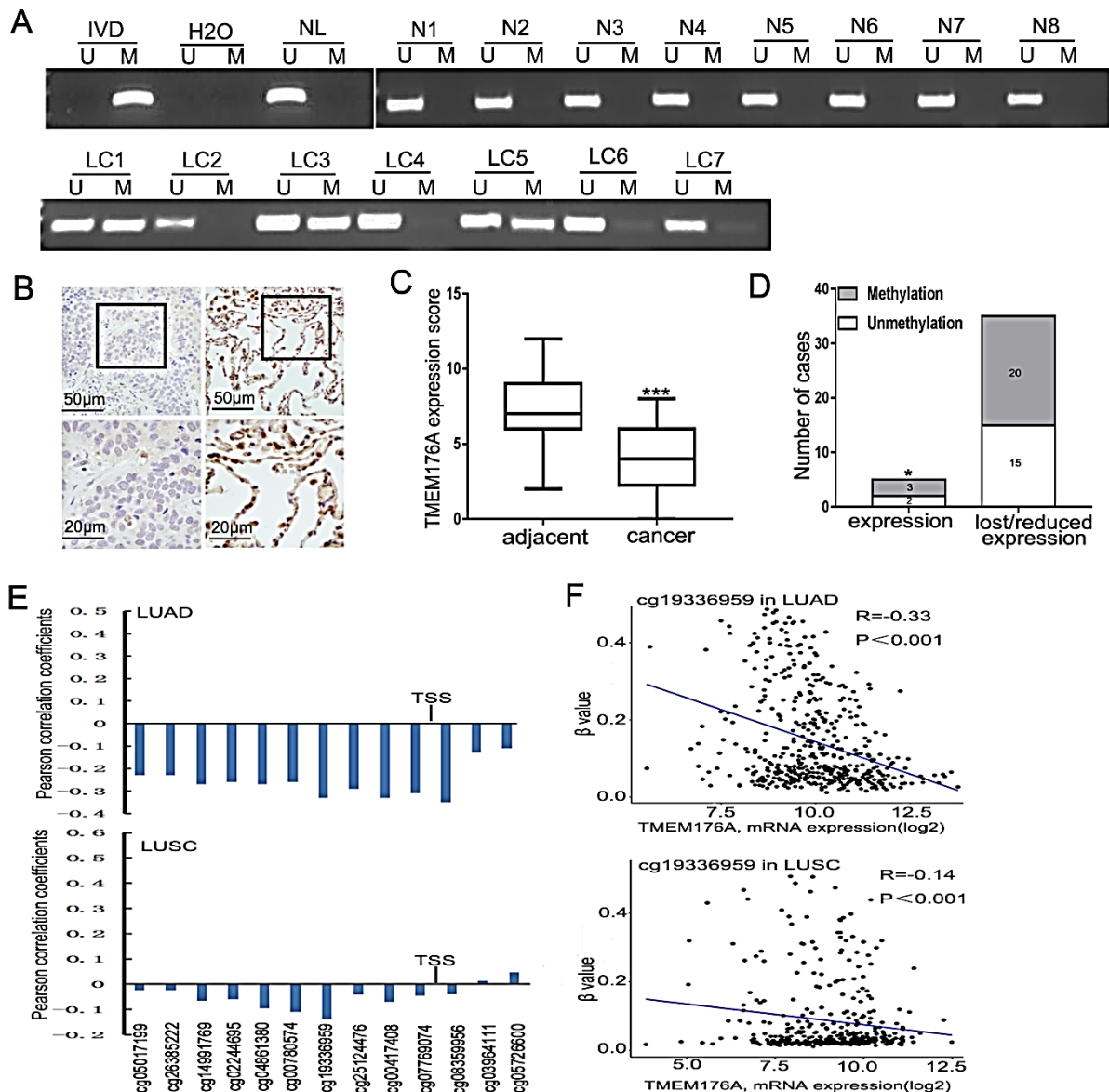


**Figure 2:** Expression and methylation status of TMEM176A in primary lung cancer. **A)** Representative MSP results of TMEM176A in normal liver tissue samples and primary lung cancer samples. N: normal liver tissue samples; LC: primary lung cancer samples. **B)** Representative IHC results show TMEM176A expression in lung cancer tissue and adjacent tissue samples (top:  $\times 200$ ; bottom:  $\times 400$ ). **C)** TMEM176A expression scores are shown as box plots, horizontal lines represent the median score; the bottom and top of the boxes represent the 25<sup>th</sup> and 75<sup>th</sup> percentiles, respectively; vertical bars represent the range of data. Expression of TMEM176A was significantly different between adjacent tissue and lung cancer tissue in 40-matched lung cancer samples.  $***P < 0.001$ . **D)** The expression of TMEM176A and DNA methylation status is shown as a bar diagram.  $*P < 0.05$ .

**E)** Pearson correlation coefficient between TMEM176A methylation and expression at each CpG site. LUAD: lung adenocarcinoma, LUSC: lung squamous carcinoma, TSS: transcription start site. **F)** Scatter plots showing the methylation status of the seventh (cg03964111) CpG sites, which are correlated with loss or reduced TMEM176A expression in 457 cases of lung adenocarcinoma samples and 372 cases of lung squamous carcinoma samples.  $\beta$ -value were considered methylated. \*\*\* $P < 0.001$ .

**II TMEM176A Inhibits Lung Cancer Cells Proliferation**

MTT and colony formation assays were used to evaluate the effects of TMEM176A on cell proliferation. TMEM176A stably expressed cells were established by transfection assay and TMEM176A highly expressed cells were knocked down by siRNA. The OD values were  $0.648 \pm 0.006$  vs.  $0.527 \pm 0.005$  in H23 cells ( $P < 0.001$ ) and  $0.878 \pm 0.010$  vs.  $0.700 \pm 0.008$  ( $P < 0.001$ ) in H1299 cells before and after restoration of TMEM176A expression (Figure 3A). The OD values were reduced significantly after the restoration of TMEM176A expression in H23 and H1299 cells (both  $P < 0.001$ ). The OD values were  $0.550 \pm 0.040$

vs.  $0.673 \pm 0.025$  ( $P < 0.001$ ) in H727 before and after knockdown of TMEM176A (Figure 3A). The OD values increased significantly after knockdown of TMEM176A expression in H727 cells ( $P < 0.001$ ). These results demonstrated that TMEM176A inhibits cell proliferation in lung cancer cells. The clone numbers were  $99.6 \pm 3.5$  vs.  $42.0 \pm 7.5$  ( $P < 0.001$ ) in H23 cells and  $128.7 \pm 5.9$  vs.  $47.7 \pm 5.7$  ( $P < 0.05$ ) before and after restoration of TMEM176A expression (Figure 3B). The clone numbers were  $26 \pm 7.9$  vs.  $71.3 \pm 11.3$  in H727 cells before and after knockdown of TMEM176A (Figure 3B). These data suggest that TMEM176A suppresses cell growth in lung cancer.

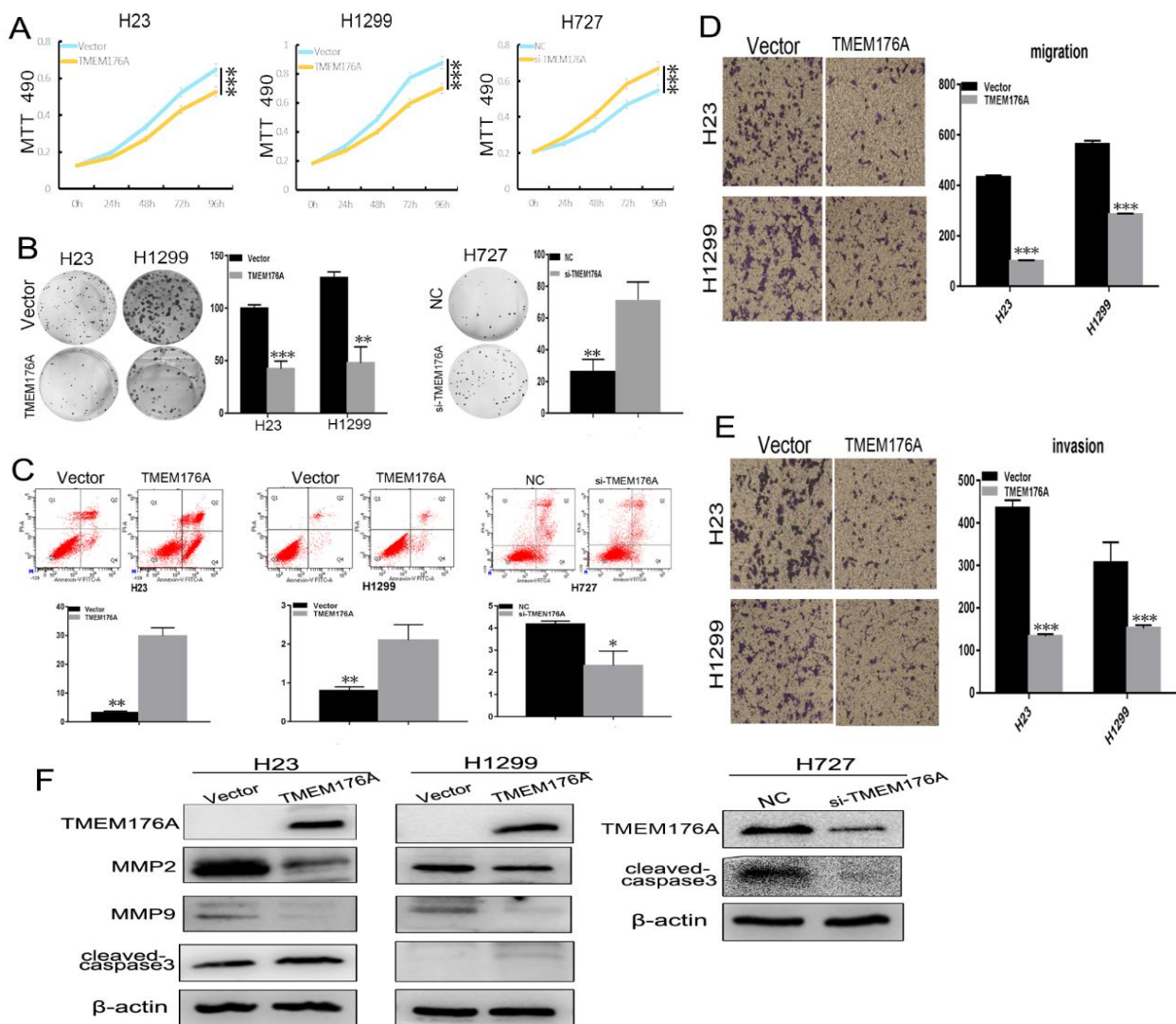


**Figure 3:** Effect of TMEM176A on lung cancer cell proliferation, apoptosis, invasion and migration. **A)** Growth curves represent cell viability analyzed by the MTT assay in TMEM176A re-expressed and unexpressed H23 and H1299 cells, as well as in H727 before and after knockdown of TMEM176A. Each experiment was repeated in triplicate. \*\*\* $P < 0.001$ . **B)** Colony formation results show that colony numbers were reduced by re-expression of TMEM176A in H23 and H1299 cells, while they were increased by knockdown of TMEM176A in H727 cells. Each experiment was repeated in triplicate. Average number of tumor clones is represented by bar diagram. \*\* $P < 0.01$ , \*\*\* $P < 0.001$ . **C)** Flow cytometry results show induction of apoptosis by re-expression of TMEM176A in H23 and H1299 cells, while reduction of apoptosis was found after knockdown of TMEM176A in H727 cells. \* $P < 0.05$ , \*\* $P < 0.01$ . **D)** The

migration assays show migration cells before and after restoration of TMEM176A expression in H23 and H1299 cells. \*\*\* $P < 0.001$ . E) The invasion assays show invasive cells before and after restoration of TMEM176A expression in H23 and H1299. \*\*\* $P < 0.001$ . F) Western blots show the effects of TMEM176A on the levels of MMP2, MMP9 and cleaved caspase-3 expression in H23, H1299 and H727 cells. Vector: control vector, TMEM176A: TMEM176A expressing vector,  $\beta$ -actin: internal control. NC: siRNA negative control; siTMEM176A: siRNA for TMEM176A.

### III TMEM176A Induces Lung Cancer Cells Apoptosis

The effect of TMEM176A on apoptosis was analyzed by flow cytometry. Under doxorubicin treatment, the ratios of apoptotic cells in TMEM176A un-expressed and re-expressed cells were  $3.2 \pm 0.01\%$  vs.  $29.8 \pm 0.03\%$  in H23 cells, and  $0.8 \pm 0.00\%$  vs.  $2.1 \pm 0.00\%$  in H1299 cells. The ratio of apoptotic cells increased significantly after the re-expression of TMEM176A (all  $P < 0.05$ , Figure 3C). In H727 cell, the ratios of apoptotic cells were  $4.17 \pm 0.00\%$  vs.  $2.30 \pm 0.01\%$  before and after knockdown of TMEM176A. The ratio of apoptotic cells decreased significantly after knockdown of TMEM176A ( $P < 0.05$ , Figure 3C). To further validate the effect of TMEM176A on apoptosis, cleaved caspase-3 expression was analyzed in lung cancer cells. The levels of cleaved caspase-3 increased after re-expression of TMEM176A in H23 and H1299 cells and decreased after knockdown of TMEM176A in H727 cell (Figure 3F). These results demonstrate that TMEM176A induces apoptosis in lung cancer cells.

### IV TMEM176A Inhibits Lung Cancer Cell Migration and Invasion

To evaluate the effects of TMEM176A on cell migration and invasion, transwell assays were used. The numbers of migration cells were  $431.5 \pm 8.22$  vs.  $98.0 \pm 4.83$  in H23 cells and  $562.0 \pm 15.03$  vs.  $285.0 \pm 3.46$  in H1299 cells before and after the restoration of TMEM176A expression. The number of migration cells decreased significantly after the re-expression of TMEM176A in H23 and H1299 cells (both  $P < 0.001$ , Figure 3D). The numbers of invasion cells were  $434.8 \pm 18.60$  vs.  $133.3 \pm 5.40$  in H23 cells and  $306.7 \pm 48.21$  vs.  $152.0 \pm 7.30$  in H1299 cells

before and after the restoration of TMEM176A expression. The cell number decreased significantly after the re-expression of TMEM176A in H23 and H1299 cells (both  $P < 0.001$ , Figure 3E). These results suggest that TMEM176A suppresses lung cancer cell migration and invasion. To further explore the mechanism of TMEM176A on cell migration and invasion, MMP2 and MMP9 expression were measured by Western blot. The expression levels of MMP2 and MMP9 were reduced after re-expression of TMEM176A in H23 and H1299 cells. These results suggest that TMEM176A inhibits cell invasion in lung cancer cells (Figure 3F). As H727 is carcinoid cell, the invasive and migratory ability are very poor. Therefore, the transwell assay was not performed.

### V TMEM176A Inhibits ERK Signaling Pathway in Lung Cancer Cells

TMEM176A was found involved in ERK signaling in our previous study in hepatic cancer [19]. The function of TMEM176A in ERK signaling was analyzed in human lung cancer. The levels of total ERK1/2 and phosphorylated ERK1/2 (p-ERK1/2) were detected by Western blot in lung cancer cells with or without TMEM176A expression. As shown in (Figure 4A), though the levels of ERK1/2 were not apparently different before and after re-expression of TMEM176A in H23 and H1299 cells, the levels of p-ERK1/2 were reduced after re-expression of TMEM176A in H23 and H1299 cells. The levels of ERK1/2 in TMEM176A highly expressed H727 cells were similar to TMEM176A knocking down cells by siRNA, while the levels of p-ERK1/2 were increased after knockdown of TMEM176A in H727 cells. These results suggest that TMEM176A inhibits ERK signaling in lung cancer cells.

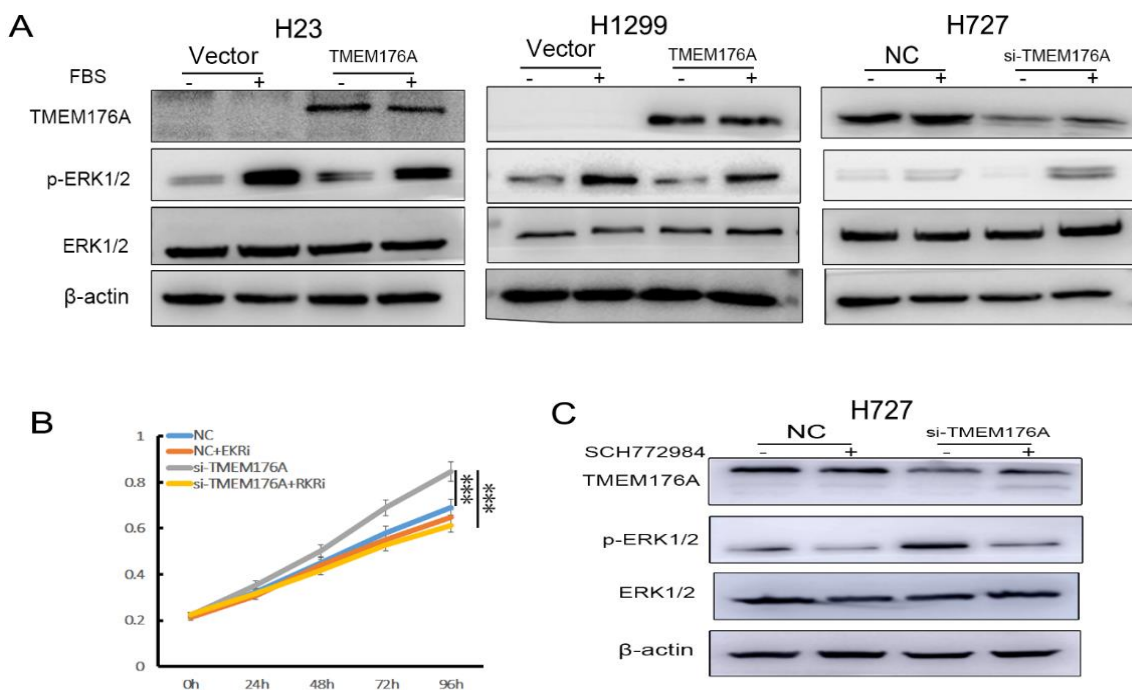




**Figure 4:** TMEM176A inhibits the ERK signaling pathway. **A)** Western blots show the levels of TMEM176A, ERK1/2 and p-ERK1/2 in H23, H1299 and H727 cells.  $\beta$ -actin: internal control. -: no serum stimulation. +: serum stimulation. **B)** Growth curves represent cell viability evaluated by MTT assay in the control group, control plus SCH772984 treatment, siTMEM176A group, and siTMEM176A plus SCH772984 treatment group in H727 cell. siTMEM176A: siRNA knockdown of TMEM176A. \*\*\* $P < 0.001$ . **C)** The expression levels of TMEM176A, ERK1/2 and p-ERK1/2 were detected by Western blot. SCH772984: p-ERK1/2 inhibitor; (-): absence of SCH772984; (+): presence of SCH772984.

To further validate the above results, MTT assay and ERK1/2 signaling inhibitor (SCH772984) were employed. The OD values were  $0.692 \pm 0.011$ ,  $0.650 \pm 0.011$ ,  $0.848 \pm 0.019$  and  $0.614 \pm 0.025$  in control group, control group plus SCH772984 treatment, siTMEM176A group and siTMEM176A plus SCH772984 treatment group in H727 cells, respectively. No significant difference was found between control group, control group plus SCH772984 and siTMEM176A plus SCH772984

treatment group (both  $P > 0.05$ ) in H727 cells. While, the OD value is reduced significantly in siTMEM176A plus SCH772984 treatment group compared to siTMEM176A group in H727 cells ( $P < 0.001$ , Figure 4B). P-ERK1/2 is reduced significantly in plus SCH772984 treatment group (Figure 4C). The above results further validated that TMEM176A inhibits ERK signaling in lung cancer.

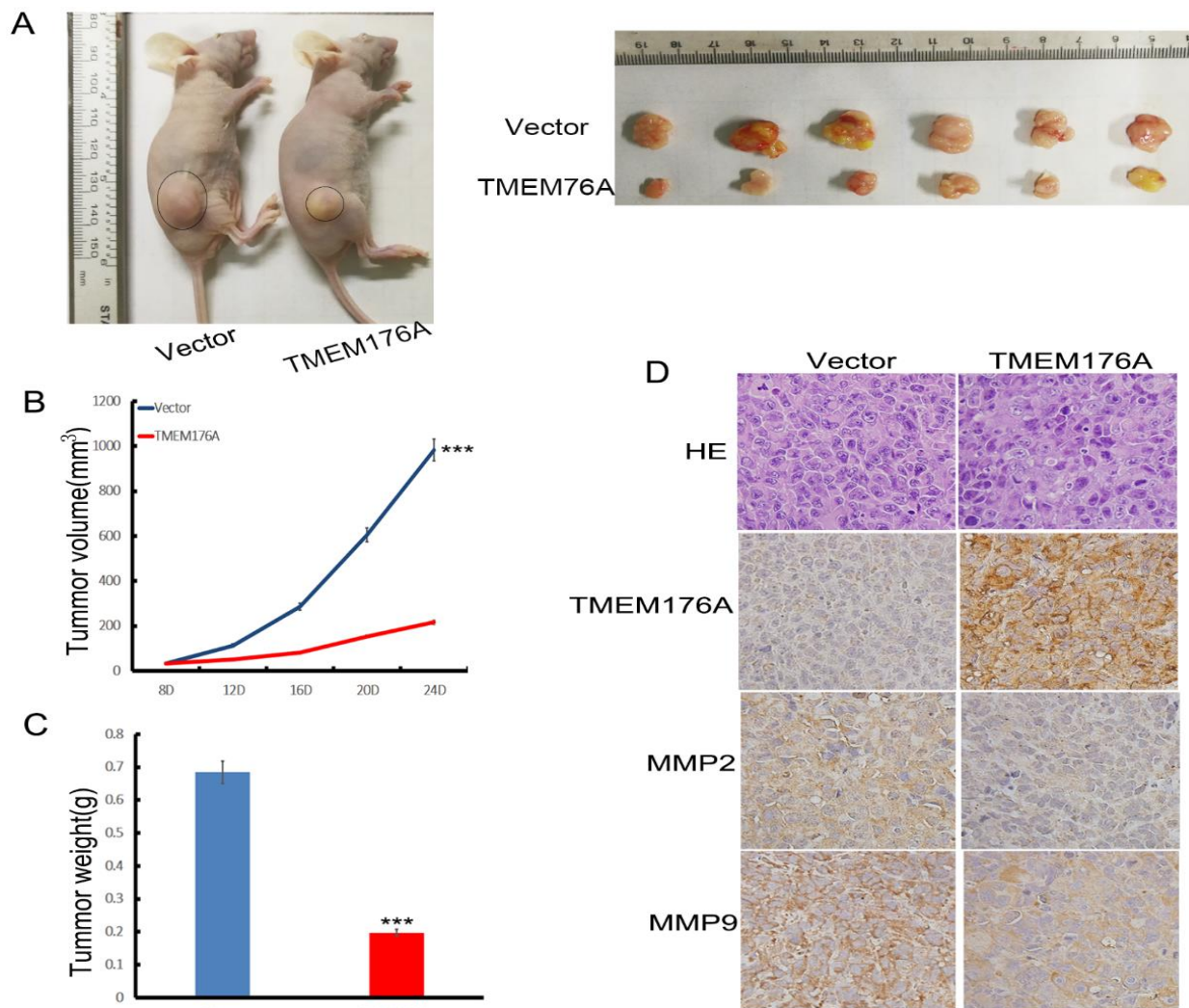


**Figure 5:** TMEM176A suppresses human lung cancer cell xenograft growth in mice. **A)** Representative tumors from TMEM176A un-expressed and TMEM176A re-expressed H1299 cell xenografts. **B)** Tumor growth curves of TMEM176A un-expressed and TMEM176A re-expressed H1299 cells. \*\*\* $P < 0.001$ . **C)** Tumor weights in nude mice at the 24th day after inoculation of un-expressed and TMEM176A re-expressed H1299 cells. Bars: mean of 6 mice. \*\*\* $P < 0.001$ . **D)** Images of hematoxylin and eosin staining show tumors from TMEM176A un-expressed and TMEM176A re-expressed H1299 xenograft mice. IHC staining reveals the expression levels of TMEM176A, MMP2 and MMP9 in TMEM176A un-expressed and TMEM176A re-expressed H1299 cell xenografts.

**VI TMEM176A Suppresses Human Lung Cancer Cell Xenograft Growth in Mice**

To further evaluate the effect of TMEM176A in human lung cancer, TMEM176A unexpressed and re-expressed H1299 cells were used to establish xenograft mouse models (Figure 5A). The tumor volume was  $983.32 \pm 101.76$  vs.  $216.06 \pm 86.96$  mm<sup>3</sup> in TMEM176A unexpressed

and re-expressed H1299 cell xenografts (Figure 5B). The tumor volume was reduced significantly in TMEM176A re-expressed H1299 cell xenograft mice ( $P < 0.001$ ). The tumor weight was  $0.68 \pm 0.11$  g vs.  $0.20 \pm 0.07$  g in TMEM176A unexpressed and re-expressed H1299 cell xenograft mice (Figure 5C). The tumor weight was reduced significantly in TMEM176A re-expressed H1299 cells xenograft mice ( $P < 0.001$ ). These results indicate that TMEM176A suppresses lung cancer cell growth in vivo. To further validate the effect of TMEM176A on tumor metastasis, the expression of MMP2 and MMP9 were examined by IHC in xenograft tumors. The expression levels of MMP2 and MMP9 were decreased in TMEM176A re-expressed H1299 cell xenografts compared to TMEM176A unexpressed H1299 cells (Figure 5D).

## Discussion

TMEM176A is located in human chromosome 7q36.1, a region where there is a frequent loss of heterozygosity in human cancers [28, 29]. By RNA-seq analysis, we found that the expression of TMEM176A was reduced in human colorectal cancer [18]. TMEM176A was found frequently methylated in human colorectal, esophageal and hepatic cancers in our previous studies. TMEM176A was demonstrated to be a potential tumor suppressor in these cancers, while a recent report suggests that the expression of TMEM176A was increased in primary human glioblastoma, and TMEM176A promoted glioblastoma cell proliferation by activating ERK signaling [18-20]. Authors also found that both TMEM176A and TMEM176B had increased expression in glioblastoma [30]. The results seem to be contradictory to our previous studies in other cancers [18-20].

However, our previous studies found that the expression of TMEM176A and TMEM176B are not associated in other cancers [18-20]. Drujont *et al.* found that the expression of TMEM176A had increased in TMEM176b<sup>-/-</sup> cells compared with wild type cells in Th17 cells in mice [31]. The expression pattern of TMEM176A and TMEM176B are possibly discrepant in different tissues. TMEM176A and TMEM176B may play different roles in various microenvironments. TMEM176B was not expressed in most human lung cancer cells (data not shown). TMEM176A is frequently methylated in human lung cancer and the expression of TMEM176A is regulated. Methylation of TMEM176A may serve as a potential lung cancer diagnostic marker. TMEM176A inhibits cell proliferation, invasion, migration, colony formation, and induces apoptosis in lung cancer. TMEM176A suppresses human lung cancer cell xenograft growth in mice. Further study suggests that TMEM176A suppresses lung cancer growth by inhibiting ERK signaling. TMEM176A is a potential tumor suppressor in human cancer and may serve as a targeting therapy marker.

In conclusion, TMEM176A is frequently methylated in human lung cancer. TMEM176A suppresses lung cancer growth by inhibiting the ERK signaling pathway.

## Author Contributions

HL performed the research and analyzed the data. HL wrote the manuscript. TH made substantial contributions to the conception and design of the study, FZ, HL and JH (James G. Herman) provided

manuscript and experimental advice. LH supervised the study. All authors read and approved the final manuscript.

## Funding

This work was supported by grants from National Key Research and Development Programme of China (2018YFA0208902); National Basic Research Program of China (973 Program No. 2012CB934002, 863 Program No. 2012AA02A203, 2012AA02A209); National Key Scientific Instrument Special Programme of China (Grant No. 2011YQ03013405); National Science Foundation of China (NSFC No.U1604281, 81672138); Beijing Science Foundation of China (BJSFC No. 7171008).

## Ethical Approval

This study was approved by the Institutional Review Board of the Chinese PLA General Hospital.

## Conflicts of Interest

None.

## Consent for Publication

We confirm that all authors have agreed with the submission in its present (and subsequent) forms.

## Availability of Data and Materials

The datasets analyzed for the current study are available from the corresponding author on reasonable request.

## Competing Interests

None.

## Abbreviations

**BSSQ:** Bisulfite sequencing  
**DAC:** 5-Aza-2'-deoxycytidine  
**HM450:** Illumina Infinium Human Methylation 450  
**IHC:** Immunohistochemistry  
**MSP:** Methylation specific PCR  
**RT-PCR:** Reverse transcription PCR  
**TCGA:** The Cancer Genome Atlas  
**TSS:** Transcription start sites  
**GAPDH:** Glyceraldehyde-3-phosphate dehydrogenase  
**IVD:** In vitro-methylated DNA  
**NL:** Normal lymphocyte DNA  
**LUAD:** lung adenocarcinoma  
**LUSC:** lung squamous cell carcinoma  
**NSCLCs:** non-small cell lung cancers

## REFERENCES

1. Bray F, Ferlay J, Soerjomataram I, Siegel RL, Torre LA et al. (2018) Global cancer statistics 2018: GLOBOCAN estimates of incidence and mortality worldwide for 36 cancers in 185 countries. *CA Cancer J Clin* 68: 394-424. [[Crossref](#)]
2. Reck M, Rabe KF (2017) Precision Diagnosis and Treatment for Advanced Non-Small-Cell Lung Cancer. *N Engl J Med* 377: 849-861. [[Crossref](#)]
3. Corrales L, Rosell R, Cardona AF, Martin C, Zatarain-Barron ZL et al. (2020) Lung cancer in never smokers: The role of different risk factors other than tobacco smoking. *Crit Rev Oncol Hematol* 148: 102895. [[Crossref](#)]
4. Brock MV, Hooker CM, Ota-Machida E, Han Y, Guo M et al. (2008) DNA methylation markers and early recurrence in stage I lung cancer. *N Engl J Med* 358: 1118-1128. [[Crossref](#)]
5. Guo M, Ren J, House MG, Qi Y, Brock MV et al. (2006) Accumulation of promoter methylation suggests epigenetic progression in squamous cell carcinoma of the esophagus. *Clin Cancer Res* 12: 4515-4522. [[Crossref](#)]
6. Yuan M, Huang LL, Chen JH, Wu J, Xu Q (2019) The emerging treatment landscape of targeted therapy in non-small-cell lung cancer. *Signal Transduct Target Ther* 4: 61. [[Crossref](#)]
7. Guo M, Liu S, Lu F (2006) Gefitinib-sensitizing mutations in esophageal carcinoma. *N Engl J Med* 354: 2193-2194. [[Crossref](#)]
8. Herbst RS, Morgensztern D, Boshoff C (2018) The biology and management of non-small cell lung cancer. *Nature* 553: 446-454. [[Crossref](#)]
9. Lim ZF, Ma PC (2019) Emerging insights of tumor heterogeneity and drug resistance mechanisms in lung cancer targeted therapy. *J Hematol Oncol* 12: 134. [[Crossref](#)]
10. Guo M, Peng Y, Gao A, Du C, Herman JG (2019) Epigenetic heterogeneity in cancer. *Biomark Res* 7: 23. [[Crossref](#)]
11. Guo M, Alumkal J, Drachova T, Gao D, Marina SS et al. (2015) CHFR methylation strongly correlates with methylation of DNA damage repair and apoptotic pathway genes in non-small cell lung cancer. *Discov Med* 19: 151-158. [[Crossref](#)]
12. Yu Y, Yan W, Liu X, Jia Y, Cao B et al. (2014) DACT2 is frequently methylated in human gastric cancer and methylation of DACT2 activated Wnt signaling. *Am J Cancer Res* 4: 710-724. [[Crossref](#)]
13. Gehrau R, Maluf D, Archer K, Stravitz R, Suh J et al. (2011) Molecular pathways differentiate hepatitis C virus (HCV) recurrence from acute cellular rejection in HCV liver recipients. *Mol Med* 17: 824-833. [[Crossref](#)]
14. Nakajima H, Takenaka M, Kaimori JY, Nagasawa Y, Kosugi A et al. (2002) Gene expression profile of renal proximal tubules regulated by proteinuria. *Kidney Int* 61: 1577-1587. [[Crossref](#)]
15. Zuccolo J, Deng L, Unruh TL, Sanyal R, Bau JA et al. (2013) Expression of MS4A and TMEM176 Genes in Human B Lymphocytes. *Front Immunol* 4: 195. [[Crossref](#)]
16. Condamine T, Le Texier L, Howie D, Lavault A, Hill M et al. (2010) Tmem176B and Tmem176A are associated with the immature state of dendritic cells. *J Leukoc Biol* 88: 507-515. [[Crossref](#)]
17. Grunin M, Hagbi-Levi S, Rinsky B, Smith Y, Chowers I (2016) Transcriptome Analysis on Monocytes from Patients with Neovascular Age-Related Macular Degeneration. *Sci Rep* 6: 29046. [[Crossref](#)]
18. Gao D, Han Y, Yang Y, Herman JG, Linghu E et al. (2017) Methylation of TMEM176A is an independent prognostic marker and is involved in human colorectal cancer development. *Epigenetics* 12: 575-583. [[Crossref](#)]
19. Li H, Zhang M, Linghu E, Zhou F, Herman JG et al. (2018) Epigenetic silencing of TMEM176A activates ERK signaling in human hepatocellular carcinoma. *Clin Epigenetics* 10: 137. [[Crossref](#)]
20. Wang Y, Zhang Y, Herman JG, Linghu E, Guo M (2017) Epigenetic silencing of TMEM176A promotes esophageal squamous cell cancer development. *Oncotarget* 8: 70035-70048. [[Crossref](#)]
21. Patel JD, Paz-Ares L, Zinner RG, Barlesi F, Koustenis AG et al. (2018) Pemetrexed Continuation Maintenance Phase 3 Trials in Nonsquamous, Non-Small-Cell Lung Cancer: Focus on 2-Year Overall Survival and Continuum of Care. *Clin Lung Cancer* 19: e823-e830. [[Crossref](#)]
22. Zheng R, Gao D, He T, Zhang M, Zhang X et al. (2017) Methylation of DIRAS1 promotes colorectal cancer progression and may serve as a marker for poor prognosis. *Clin Epigenetics* 9: 50. [[Crossref](#)]
23. Wang Y, Zhang Y, Herman JG, Linghu E, Guo M (2017) Epigenetic silencing of TMEM176A promotes esophageal squamous cell cancer development. *Oncotarget* 8: 70035-70048. [[Crossref](#)]
24. Yan W, Wu K, Herman JG, Brock MV, Fuks F et al. (2013) Epigenetic regulation of DACH1, a novel Wnt signaling component in colorectal cancer. *Epigenetics* 8: 1373-1383. [[Crossref](#)]
25. Jia Y, Yang Y, Liu S, Herman JG, Lu F et al. (2010) SOX17 antagonizes WNT/beta-catenin signaling pathway in hepatocellular carcinoma. *Epigenetics* 5: 743-749. [[Crossref](#)]
26. Cui Y, Gao D, Linghu E, Zhan Q, Chen R et al. (2015) Epigenetic changes and functional study of HOXA11 in human gastric cancer. *Epigenomics* 7: 201-213. [[Crossref](#)]
27. Yang MC, Lin RW, Huang SB et al. (2016) Bim directly antagonizes Bcl-xl in doxorubicin-induced prostate cancer cell apoptosis independently of p53. *Cell Cycle* 15: 394-402. [[Crossref](#)]
28. Riegman PH, Burgart LJ, Wang KK, Wink-Godschalk JC, Dinjens WN et al. (2002) Allelic imbalance of 7q32.3-q36.1 during tumorigenesis in Barrett's esophagus. *Cancer Res* 62: 1531-1533. [[Crossref](#)]
29. Kimmel RR, Zhao LP, Nguyen D, Lee S, Aronszajn M et al. (2006) Microarray comparative genomic hybridization reveals genome-wide patterns of DNA gains and losses in post-Chernobyl thyroid cancer. *Radiat Res* 166: 519-531. [[Crossref](#)]
30. Liu Z, An H, Song P, Wang D, Li S et al. (2018) Potential targets of TMEM176A in the growth of glioblastoma cells. *Oncotargets Ther* 11: 7763-7775. [[Crossref](#)]
31. Drujont L, Lemoine A, Moreau A, Bienvenu G, Lancien M et al. (2016) RORyt+ cells selectively express redundant cation channels linked to the Golgi apparatus. *Sci Rep* 6: 23682. [[Crossref](#)]